Reaction Dynamics at Liquid Interfaces

Ilan Benjamin
Department of Chemistry and Biochemistry
University of California, Santa Cruz, Santa Cruz, CA 95064
ilan@ucsc.edu

Table of Contents

1. Introduction
2. Solvation at Liquid Interfaces
    2.1. Surface solute density
    2.2. Solvation structure at liquid interfaces
3. Reactivity at Liquid Interfaces
    3.1. Introduction
    3.2. Ion transfer (IT) across the liquid/liquid interface
    3.3. Electron transfer reactions at liquid/liquid interfaces
    3.4. Liquid-Liquid Phase Transfer Catalysis and interfacial S_N2 reactions
4. Conclusions

Abstract: The liquid interface is a narrow, highly anisotropic region, characterized by rapidly varying density, polarity and molecular structure. We review several aspects of interfacial solvation and show how these affect reactivity at liquid/liquid interfaces. We specifically consider ion transfer, electron transfer and S_N2 reactions, showing that solvent effects on these reactions can be understood by considering the unique structure and dynamics of the liquid interface region.

Keywords: ion transfer, electron transfer, phase transfer catalysis, S_N2 reaction.

1. Introduction

The study of chemical reactions that take place at the interface between a liquid and a second phase (vapor, another immiscible liquid or a solid) is of major interest in science and technology. Examples include: uptake of pollutants by water surfaces, metal ion extraction, phase transfer catalysis, drug and ion transport through membranes, corrosion, solar energy conversion and water splitting reactions. Because of its importance, it is not surprising that the study of the neat liquid surface, as well as of solute adsorption, spectroscopy and reactivity, goes back many years. However, up until the last decade of the 20^{th} century most of the experimental studies involved the measurement of macroscopic properties such as surface tension and current-voltage relations (1, 2). Although these techniques have contributed significantly to our knowledge, they lack the ability to provide a detailed understanding at the molecular level.

In recent years, these long-standing experimental techniques for probing interfacial reactions have been supplemented by a number of new methods, which have provided unprecedented sensitivity and selectivity in the measurement of liquid interfacial properties and phenomena. These include varieties of non-linear spectroscopic techniques such as Second Harmonic Generation (SHG) and Sum Frequency Generation (SFG), atomic, light, X-ray and neutron scattering, scanning electrochemical microscopy and more. The description and application of these techniques have been extensively reviewed (3-11).

In parallel to the experimental progress, significant contribution to the theoretical understanding of liquid interfaces has been provided by phenomenological theories (continuum models), approximate statistical mechanical approaches and computer

simulations, but by and large these have been focused on the structure and dynamics of the neat liquid surface and interfaces, and on the adsorption of neutral and charged solute molecules at the interface. This progress has been quite extensively reviewed (12-16).

The purpose of this chapter is to review the experimental and theoretical progress made in the past 10-15 years on understanding *reactivity* at liquid interfaces. While a description of the liquid as a structure-less medium has been very useful for offering a qualitative understanding of solvent's effect on the dynamics and thermodynamics of chemical reactions, computer simulations and experiments clearly suggest that a microscopic molecular description of the solvent is important and sometimes necessary. This is particularly so at interfaces, because the interfacial region itself is only a few molecular diameters thick. Thus, the focus of this chapter is on the microscopic insight gained about the systems by contrasting the experimental observation with (mostly) molecular simulations. We specifically focus on the fundamental question: To what extent can one understand surface effects by invoking effective average medium properties (which are related to the properties of the two adjoining phases) or are there unique surface effects, which may arise from the fact that the surface region is highly inhomogeneous with extreme asymmetry in the intermolecular forces? The goal is to present unifying concepts rather than focus on details that are specific to a given system. To keep the chapter at a reasonable length we also limit our discussion to the liquid/vapor and liquid/liquid interface of simple liquids, referring the reader to recent reviews of liquid/solid interfaces (17).

2. Solvation at liquid Interfaces

Understanding the thermodynamics of interfacial solvation and the associated molecular structure and dynamics of solute molecules at liquid interfaces is of major importance for understanding their reactivity. This topic has received much attention, and our focus in this section is to summarize the current view on a number of important general concepts that will be useful for elucidating reactivity at interfaces.

2.1. Surface solute density

A basic solute thermodynamic property whose knowledge is crucial for the quantitative determination of its reactivity is its equilibrium surface concentration, and more generally, the solute density profile along the interface normal, $\rho_s(z)$. The integral of $\rho_s(z)$ along z gives the total number of solute molecules per unit area, which is typically not equal to the integral of the constant bulk density ρ_b over the same interval (which includes the interface region). The difference defines the surface excess density Γ, which at fixed temperature is related to the surface tension of the solution γ and the solute chemical potential μ via the Gibbs adsorption equation (18):

$$d\gamma = -\Gamma d\mu \qquad \text{(fixed temperature)}. \tag{1}$$

The surface excess density Γ and the surface tension can be measured as a function of the bulk solute concentration ρ_b giving the adsorption isotherm (1). If $\Gamma > 0$, the solute is considered surface-active, and according to Eq. 1, this is associated with a decrease in the surface tension relative to pure solvent(s). While the adsorption isotherm can easily be measured, the experimental determination of $\rho_s(z)$ is much more difficult, and only recently have X-ray reflectivity measurements been used as the first experimental technique to measure ion density profiles directly at the water/organic liquid interface

(19, 20). Thus, most of our knowledge of $\rho_s(z)$ has been obtained from direct sampling of solute's center of mass location via computer simulations:

$$\rho_s(z) = \left\langle \delta(z - z_{\mathrm{cm}}) \right\rangle = \frac{\int e^{-\beta H} \delta(z - z_{\mathrm{cm}}) d\mathbf{r}}{\int e^{-\beta H} d\mathbf{r}} \quad , \tag{2}$$

where z_{cm} is the center of mass of the solute along the interface normal calculated relative to the system's center of mass, and $\beta = 1/k_B T$. The solute density profile is closely related to the local free energy profile, also called the Potential of Mean Force (PMF) through (18):

$$A(z) = k_B T \ln \rho_s(z) \, , \tag{3}$$

If the solute is surface-active, $A(z)$ will typically have a minimum at some interface location z_{int}, and $\Delta A_{\mathrm{ads}} = A(z_{\mathrm{int}}) - A(z_{\mathrm{bulk}})$ is the solute adsorption free energy. It can be obtained experimentally from the adsorption isotherm (1). The PMF can also be computed directly by integrating the average total normal force on the solute center of mass (21).

The goal of the simulations of solute density profiles and PMFs has been to gain insight into the molecular structure of the interface while testing the ability of simulation methodologies and force fields to reproduce the relation between surface tension and solute surface excess. Of particular interest has been the study of ionic distributions at the water liquid/vapor interface, because of its relevance to the heterogeneous photochemistry of sea salt aerosols, a system implicated in ozone depletion. Other important contributions are studies of adsorption and transfer of solute across the water/organic liquid interface, which are motivated by applications in electrochemistry, solvent extraction and phase transfer catalysis. Excellent recent reviews of these

simulations and experiments (focusing mainly on the surface of electrolyte solutions) are available (15, 16, 22, 23).

2.2. Solvation structure at liquid interfaces

Experimental and theoretical studies over the last several decades have shown how the structure of the solvation shell in bulk solvent plays a crucial role in determining the energy flow between the solvent and solute molecules and the solute reactivity. Clearly this must also be important at liquid interfaces – both the equilibrium structure and the fluctuations from this structure. At a fundamental level, the structure may be characterized by the solute-solvent pair correlation function $\rho^{(2)}(\mathbf{r}_s, \mathbf{r}_l)$, which gives the probability of finding the solute molecule's center of mass at location $\mathbf{r}_s$, given a solvent molecule at $\mathbf{r}_l$. In a bulk homogeneous liquid, $\rho^{(2)}(\mathbf{r}_s, \mathbf{r}_l)$ is only a function of the solvent-solute distance $r = |\mathbf{r}_s - \mathbf{r}_l|$ and is proportional to the solvent-solute radial distribution function $g_{sl}(r)$. However, at a planar interface $\rho^{(2)}(\mathbf{r}_s, \mathbf{r}_l)$ is a function of r, z (the solute's center of mass location) and the angle θ between the vector $\mathbf{r}_s - \mathbf{r}_l$ and the interface normal. Computer simulations have provided the only direct information about $\rho^{(2)}(\mathbf{r}_s, \mathbf{r}_l)$, although some experimental information is becoming available. In this respect, we note the recent report of the hydration structure of bromide ions at the 2-octanone/water interface using total-reflection X-ray absorption fine structure (24).

To simplify the description, the three dimensionality of the pair correlation is typically reduced by averaging $g_{sl}(r, z, \theta)$ over θ with the solute's center of mass restricted to a slab of some small width (a few Å) centered at z, giving the more manageable one-dimensional $g_{sl}(r; z)$. At liquid/liquid interfaces, this function can be

calculated for each of the two immiscible solvents. Further reduction of this quantity is possible by integrating $g_{sl}(r; z)$ up to its first minimum ($r_{\min}$) to obtain the number of solvent molecules in the first solvation shell as a function of z:

$$n(z) = \int_0^{r_{\min}} \rho_{bulk} g_{sl}(r;z) 4\pi r^2 \, dr \, . \tag{4}$$

Molecular dynamics studies (25-30) of the hydration structure of spherical solutes of various sizes and charges at the water liquid/vapor interface and at water/immiscible liquid interfaces provide a useful general concept that is demonstrated in Fig. 1. This figure shows $n(z)$ relative to its value in bulk water at the water liquid/vapor interface for Li^+ (small ion) and I^- (large ion) and for fictitious particles identical to Li^+ and I^- in their size, but with no charge. The small ion is able to keep its hydration shell intact when it is moved to the liquid/vapor interface. The ability of the larger ion to do this is significant, but somewhat diminished. In contrast with the case of charged particles, there is a significant depletion in the number of water molecules in the first hydration shell of the neutral atoms. We note but do not show that in all cases the second hydration shell is diminished significantly as the solute is transferred to the interface. This similarity in bulk and interfacial behavior was also noted recently for OH^- and for the hydrated electron (31).

As will be discussed below, the semi-invariance of the ion's hydration structure manifests itself during ion transfer across the liquid/liquid interface. Depending on its size and charge, the ion is able to drag all or part of its hydration shell as it is transferred from the aqueous to the organic phase (28, 32-40). Closely related to this concept is the

role played by the fluctuations in the solvent-ion interactions in driving small ions towards and away from the interface (41).

The above picture is essentially unchanged for small polar and ionic molecules. For example, Table 1 compares the peak values of $g_{X\text{-}O}(r; z)$ in bulk and surface water and acetonitrile when X is the iodine atom in the I_2^- and I_2 molecules or the Cl atom in OCl and OCl^- molecules. Neutral molecules exhibit a much greater decrease in the peak of the radial distribution function (by a factor of about 3) compared with ionic solute. And, as in the case of atomic ions, the degree to which the first solvation shell remains intact increases with a decrease in the ion size.

An important consequence of a nearly complete hydration shell around ions at water interfaces is the marked similarity between the bulk and surface rotational and vibrational relaxation rates as demonstrated by simulations, and the similarity between the bulk and surface solvation dynamics as demonstrated by simulations and experiments. We refer the reader to recent reviews of these topics (44, 45).

3. Reactivity at Liquid Interfaces

3.1. Introduction

The characteristic molecular structure and dynamics of liquid interfaces -- namely, a narrow region, asymmetry in intermolecular interactions, specific molecular orientation, and density fluctuations -- influence solvation structure, solvation thermodynamics and dynamics, and it is expected to influence the rate and equilibrium of interfacial chemical reactions. While one can also approach solvent effects on interfacial reactions at a continuum level by considering how the variation in density, viscosity and dielectric response influences reactivity, studies of chemical reaction dynamics and

thermodynamics in bulk liquids have demonstrated that the solvent should be viewed as an active participant whose molecular structure must be considered to fully understand solvation and reactivity (46-50).

Below we examine recent progress in understanding at the molecular level the dynamics and thermodynamics of several processes of importance to interfacial reactivity. We focus on two important general questions:

a) How does the interface region affect the rate and equilibrium of different types of reactions?

b) Can solvent effects on reactions at interfaces be understood by using properly scaled/modified bulk liquid concepts, or are there unique surface effects?

Most of our understanding of surface reactivity has been obtained by new experimental methodologies specifically designed to probe the interface region and from computational approaches that typically involve applications of methods developed for the study of reactivity in bulk liquids (46-49). As some of these studies have been previously reviewed (51, 52), we provide only a brief update of those topics and discuss in greater detail topics that have not yet been reviewed.

3.2. Ion transfer (IT) across the liquid/liquid interface

Although not a chemical reaction in the usual sense, the transfer of ions across the interface between two immiscible electrolyte solutions shares important characteristics with typical charge transfer reactions. The electrochemical experimental techniques, both classical and those recently developed to measure the rate of IT, have also been used to measure the rate of electron transfer (ET) across the interface. Some attempts to describe the IT process as an activated crossing of a barrier have been made. Several types of

chemical reactions such as ET, nucleophilic substitution and phase transfer catalysis discussed below are coupled to IT, so the study of "pure" IT should help in analyzing these reactions. Early work on IT has been reviewed (2, 53). Recent excellent reviews of this topic include those by Dryfe (54), a book chapter by Mirkin(55) and articles by Dassie and coworkers (56) and by Scholz (57). In discussing IT, it is useful to separate the thermodynamics and kinetic/mechanistic aspects of the transfer process.

3.2.1. Thermodynamics

The fundamental question about thermodynamics of IT is the determination of ΔG_t, the standard free energy of IT between two immiscible liquids, typically water and an organic solvent, and the related problem of the electric potential change across the interface due to the partitioning of the ions in the two immiscible solutions (54). The assignment of absolute values of ΔG_t for single ions is complicated by the need to use an extra-thermodynamic assumption to separate the contributions of the anion and cation (typically, the anion and cation of tetraphenylarsonium tetraphenylborate are assume to have the same value of ΔG_t) and by experimental difficulties such as ohmic resistance of the organic phase. Nevertheless, significant progress has been made on the experimental front, which has been recently reviewed (55-57).

Some of the important recent advancements and results that should be pointed out are the use of three-phase electrodes to study the transfer of ions between water and a low polarity organic solvent such as *n*-octanol (57) and the use of ultramicroelectrodes and a scanning electrochemical microscope to minimize ohmic drop (55). These techniques and other variations on classical techniques have produced a wealth of data on the free energy of transfer of simple and complex ions with a large number of different solvents. While

the most common solvent pairs studied are water/1,2-dichloroetahne and water/nitrobenzene, other solvents, including ionic liquids, have been studied. Hundreds of references and tables for these values are given in the recent review of Dassie and coworkers (56).

The fundamental theoretical challenge is to predict the value of the free energy of transfer from the properties of the ions (size, charge and polarizability) and the two solvents. More generally knowledge of the full free energy profile (potential of mean force – PMF , see eq. 3) is sometimes necessary for correct interpretation of experiments. The two main approaches used are continuum electrostatic models of varying sophistication and molecular dynamics/Monte Carlo simulations.

PMF calculations of ion and solute transfer across the water/immiscible liquid interface generally show a monotonic change between the two phases (13, 19, 20, 33-38, 58-61). The net change in the PMF: G(bulk liquid) – G(bulk water) = $\Delta G_{transfer}$, gives the Gibbs free energy of transfer from the water to the immiscible liquid phase. Results are in qualitative agreement with experimental data and with continuum electrostatic models (13, 62), although in the latter case adjustable parameters (the size of the spherical cavity used to model the ion) were needed to obtain a good fit (13).

While most comparisons of the free energy profile between experiments and simulations have been limited to just the net free energy of transfer, X-ray reflectivity measurements can probe the total ionic density across the interface between two immiscible electrolyte solutions and can be used to make a comparison with the full PMF. The PMF of Br^- and tetra butyl ammonium cation (TBA^+) across the water/nitrobenzene interface, calculated by MD, have been used to derive the ionic

density distribution. The total distribution was found to agree well with the measured one over a wide range of bulk electrolyte concentrations (19, 20). This contrasts with the predictions of the continuum electrostatic Gouy-Chapman theory, where ionic density distributions vary substantially from the X-ray reflectivity measurements, and this underscores the importance of molecular-scale structure at the interface.

Of course, if one is only interested in the net free energy of transfer, then calculating the full PMF is not necessary. Instead, one may calculate the absolute free energy of solute solvation in the bulk of each solvent and simply take the difference. This however, ignores the possibility that ions (especially small hydrophilic ones) may retain a partial hydration shell while being transferred into the organic phase. This approach was demonstrated for the free energy of transfer of alkali and halide ions from water to 1,2-dichloroethane (DCE). Free energy calculations of different sized ion-water clusters (different numbers of water molecules) in bulk DCE (63) reproduce the free energy of transfer (ΔG_t) of ions from water to this solvent, in reasonable agreement with the experimental data. Accounting for the possibility of ions retaining part of their hydration shell is critical for the correct interpretation of several dynamical phenomena such as vibrational and rotational relaxation and solvation dynamic, as reviewed elsewhere (45).

3.2.2. Kinetics

The rate of ion transfer across the liquid/liquid interface has mainly been studied by electrochemical means (cyclic voltammetry, AC impedance, scanning electrochemical microscopy and others). An applied external field or an ionic concentration gradient across the interface is established and the resultant current is measured. The experimental data can be represented by a first-order rate constant if the transfer process is written as a chemical reaction:

$$I^{z_i}(w) \rightleftarrows I^{z_i}(o) \quad , \tag{5}$$

where z_i is the ionic charge, and *w* and *o* correspond to the aqueous and organic phase, respectively. This equation applies to any ion that can transfer between the two phases. The contribution of ion *i* to the total current density *J*(coulomb/cm^2) can then be written:

$$J_i = z_i F(k^i_{w\to o} c^w_i - k^i_{o\to w} c^o_i) \quad , \tag{6}$$

where *F* is Faraday's constant, c^w_i and c^o_i are the ion concentration in the two phases, and $k^i_{w\to o}$ and $k^i_{o\to w}$ are the forward and backward rate constants, respectively (units of velocity, cm/sec). Since the concentrations can be related to the potential drop across the interface and the equilibrium concentration to the standard free energy of transfer, one can derive a relation between the external potential and the current and use experimental current-potential data to extract the rate constants. The fundamental experimental challenge of the past 2.5 decades is that the apparent values of these rate constants depend on the method used to measure them with values (for the same ion and solvents) varying over 4 orders of magnitudes. The reason for this is only partially understood and possibly includes uncompensated ohmic drop across the organic phase, which leads to uncertainty in the value of the potential drop across the interface, inappropriate instrument time resolution, and inadequate separation of time scales between the ion transfer rate and the time it takes to establish the double-layer potential. When a reason is suspected, ingenious new experimental approaches to overcoming the problem have been devised. A more complete discussion of this problem and the attempts to tackle it can be found in recent reviews (54, 55).

Given the uncertainty in the values of rate constants, a theory for predicting such rates may seem premature at present. Such a theory will depend on a reasonable answer

to the fundamental question about the mechanism of ion transfer: Can it be thought of as a diffusion in an external field or as an activated crossing of a barrier, or perhaps involve aspects of both?

While theoretical models for ion transfer based on the Nernst-Planck equation (diffusion in an external field) or transition state theory of charge transfer were developed early on, molecular dynamics simulations have provided the first qualitative molecular insight into the process, which in turn has resulted in several recent improvements to the early models. The recent review by Dryfe (54) provides an excellent description of this work up to 2007, which we briefly summarize before describing some recent developments.

The standard modeling of ion transfer by coupling of the diffusion equation to the Nernst equation is well established (64) and extensively used to simulate cyclic voltammetry experiments in order to extract rate constants. Typically, however, little molecular insight is directly gained from this description. A solution of the diffusion equation with an external field, which includes the ion potential of mean force (determined from MD or MC simulations) in addition to the applied potential, can add some molecular insight. A starting point for this description is the Nernst-Planck equation, whose differential form is

$$\frac{\partial c_i}{\partial t} = \frac{\partial}{\partial z}\left[D\frac{\partial c_i}{\partial z} + \frac{Dq_i c_i}{k_B T}\frac{\partial \phi}{\partial z}\right] \tag{7}$$

where D is the diffusion constant (could taken to be distance-dependent) $\phi(z)$ is the electrochemical potential variation and q_i the charge of the ion. A numerical solution of this equation with the electrochemical potential set equal to the MD-derived PMF was

compared with direct MD trajectory calculations of ion transfer across a model liquid/liquid interface (65). The good agreement found suggests that in this case, a diffusive description of the IT process is reasonable. However, rate constants derived from this equation using plausible values for D, the gradient of ϕ and the size of the interface region give rate constants values that are two order of magnitude larger than measured (54, 66). The slower rate constant suggests a barrier or some type of retardation effects.

If the potential of mean force exhibits a barrier, one may calculate the rate constant using transition state theory or equivalent methods. An example of this approach was provided by Schmickler employing a lattice gas model (67). His calculations show that in most cases the current voltage relations follow a Butler-Volmer type law.

In the above approaches, the solvent provides a mean field for the ion motion, and fluctuations are ignored. However, molecular dynamics simulations of ion transfer under the influence of an external field (32, 33, 35), several recent simulations, (e.g. (68)) and the equilibrium calculations of ionic solvation structure discussed earlier suggest the importance of water molecules' protrusions (water "fingers") into the organic phase (which can be thought of as localized capillary waves) as a mechanism that can enhance ion transfer rate into the aqueous phase and inhibit the reverse process. Marcus presented a theoretical model to quantify the contributions of these fluctuations (69), estimating the rate of ion attachment and detachment from a water "finger" and diffusion along it. He concluded that the rate-limiting step is likely the motion of the ion along a "solvation coordinate".

The MD simulations mentioned above also suggest that the coupling of ion motion and solvent dynamics at interfaces can result in solvent "fingers" produced in response to the ion approaching the interface. A two-mode Langevin model, in which one degree of freedom describes the ion motion and a second one describes interface dynamics, was proposed by Urbakh and co-workers. It was solved analytically and numerically over a range of ion-surface couplings (70, 71). The analytical expression derived for the rate constant of IT suggests that this coupling can result in a slowing down of the ion motion relative to unhindered simple diffusion.

A molecular level approach for describing the collective surface interaction with the ion using a single (or a few) degree(s) of freedom ("solvation coordinate") was suggested by Schweighofer and Benjamin (33). In this approach, two solvation coordinates s_{W} and s_{L} are defined by dividing the instantaneous interaction energy between the ion and the two solvents (with W representing the water and L the second immiscible liquid) by the average interaction energy of this ion in the bulk of each solvent:

$$\begin{aligned} s_{\mathrm{W}} &= U_{ion-water}(z) \big/ \left\langle U_{ion-water}(\text{bulk water}) \right\rangle \\ s_{\mathrm{L}} &= U_{ion-liquid}(z) \big/ \left\langle U_{ion-liquid}(\text{bulk liquid}) \right\rangle \end{aligned} \quad . \tag{8}$$

One expects:

$$s_W(z \to \text{bulk water}) = 1,\ s_W(z \to \text{bulk liquid}) = f \quad , \tag{9}$$

where $f < 1$ represents the interaction of the ion with the fraction of the hydration shell that was co-transferred to the organic phase ($f = 0$ for a hydrophobic ion). Insight into the mechanism of the transfer may be obtained by following the IT dynamics on a two-dimensional s_{W}-z surface, as well as computing the two-dimensional free energy surface

$G(s_W, z)$. This approach was recently applied (72) to the transfer of tetra-alkyl ammonium ions and ions pairs across the water/chloroform interface. It is interesting to note that for the several ions considered in this work it was found that $\langle s_W(z)\rangle + \langle s_L(z)\rangle \approx 1$, with the angular bracket representing equilibrium average while the ion is constrained to a narrow slab centered at the location z. It would be useful to check the validity of this "conservation law" for a wide range of liquids and ions.

The transfer of ions across the interface must involve some exchange of the solvent molecules around the ion. Understanding the mechanism and dynamics of this process is surely necessary for a quantitative understanding of the IT process, for elucidating the nature of "finger" formations and for the possible existence of any barrier. While several studies examined the perturbation of the water structure upon ion transfer (68, 72), the only reported dynamical study is an examination of the rate (and mechanism) of hydration shell exchange dynamics during the transfer of Na^+ and Li^+ between water and nitrobenzene (28). As the ions are transferred from the water to the organic phase, they keep their first hydration shell and an incomplete second shell. The rate of water exchange between the first shell and the rest of the interfacial water molecule decreases during the transfer, which is consistent with an increase in the barrier along the ion-water potential of mean force. The study also examines some aspects of the exchange mechanism, but clearly much more work is needed here.

We conclude by noting that ion pairing could play a role in the transfer process. For example, Mirkin and coworkers suggested a "shuttle" mechanism to explain the observation that a very low concentration of a supported electrolyte in the organic phase facilitates the transfer of hydrophilic cations (73).

3.3. Electron transfer reactions at liquid/liquid interfaces

Electron transfer (ET) at the interface between two immiscible electrolyte solutions (IES) is a fundamental process with important implications for solar energy conversion (74), phase transfer catalysis and biological processes at membrane interfaces (75). The experimental and theoretical study of ET reactions at IES interfaces has a long history (2). Until about 15 years ago, measurements of ET rates at IES involved mainly conventional electrochemical methods, where the interface was under external potential control and a steady state current vs. voltage was measured (2, 53). These measurements suffered from several drawbacks, such as an inability to distinguish clearly between electron and ion transfer, distortion due to the charging current and the large resistivity of the organic phase. These drawbacks limit the number of experimental systems that can be studied, and thus very few reliable rate constants have been reported.

Recent experimental developments in which those drawbacks can be minimized or controlled have provided new data that helped clarify the factors that control ET at IES and test several theories. These new techniques include scanning electrochemical microscopy (SECM) (76), thin-layer cyclic voltammetry (77) and spectro-electrochemical methods (78-80), some taking advantage of recent advances in non-linear optics (81, 82). These have been reviewed recently (54, 55).

Like ET in bulk solvents, ET at a L/L interface is a bimolecular reaction but with the ability to control the reaction free energy (ΔG_{rxn}) by an applied potential like an ET at the electrolyte/electrode interface. The typical case is when the acceptor and donor (O_1 and R_2) are located in the two opposite phases, so the reaction can be written as follows:

$$O_1(w) + R_2(o) \rightleftarrows R_1(w) + O_2(o) \quad . \tag{10}$$

The rate of this reaction can be obtained by applying a potential difference V across the interface and measuring the current I. Extracting the forward and backward rate constants from this measurement requires a theoretical framework. In turn, this theoretical framework is based on knowledge/assumptions about the interface structure, ionic distributions and variation of the electric potential across the interface.

The basic theory of ET in bulk liquids and at liquid/metal interfaces is well-developed (83-86). By making some assumptions about the interface structure and ionic distributions, Marcus has derived an expression (see below) for the rate constant's dependence on the reaction free energy (and thus the external potential). This relation leads to the phenomenological Butler-Volmer equation:

$$I = I_0\left(e^{(1-\alpha)nF(V-V_{eq})/RT} - e^{anF(V-V_{eq})/RT}\right) \tag{11}$$

where T is the temperature ,R is the gas constant, F is the Faraday constant, n is the number of electrons transferred, V_{eq} is determined from the Nernest equation and the activities of the oxidized and reduced ions at the interface, α is a constant called the transfer coefficient (see below), and I_0 is directly related to the forward heterogeneous rate constant k_f by:

$$I_0 = nF\left[\mathrm{O}_1\right]^{1-\alpha}\left[\mathrm{R}_2\right]^{\alpha} k_f\,, \tag{12}$$

where $[O_1]$ and $[R_2]$ are the equilibrium concentrations. Marcus derivation (83) shows that the transfer coefficient is given by $\alpha = 1/2 + \Delta G_{rxn}/2\lambda$, where ΔG_{rxn} is the reaction free energy, and λ is the reorganization free energy (see below).

Some experiments were found to follow this relation, from which one can extract the rate constant, but some others seems to show only weak current-potential dependence

(77, 87). A summary of the experimental situation until 2007 is provided by Dryfe (54) and more recently by Mirkin (55).

The breakdown of the Butler-Volmer relation could be due to the failure of one or more of the assumptions on which this equation is based: 1) the validity of Marcus theory (see next section); 2) the potential drop across the interface is assumed to be equal to that imposed on the electrodes (or an account can be made for the contribution of the layers of inert ions using the Nernst equation(88)); 3) the current due to ion transfer is small (or it can be accounted for). While assumptions 2 and 3 can be addressed to some degree by experimental advances, like SECM (76), theoretical developments have played a role in examining Marcus theory, which we briefly discuss next.

3.3.1. Marcus non-adiabatic theory of ET at IES interfaces

In the limit of weak electronic coupling between a donor and acceptor separated by a distance *R* and adsorbed at the liquid-liquid interface, the bi-molecular rate constant for an electron transfer reaction was derived by Marcus (89-91):

$$k_r = \kappa \nu V_r e^{-\beta \Delta G^*} \quad , \tag{13}$$

where ν is a "collision" frequency, which is determined from the equilibrium solvent fluctuations in the reactant state, V_r is the reaction volume, which accounts for all of the possible configurations of the reactant pair per unit area of the interface, and ΔG^* is the activation free energy. The Landau-Zener (LZ) factor κ, which is proportional to the square of the electronic coupling term V_{el}, determines the probability for the electronic transition. (For a recent discussion of the LZ factor, see (92)). A basic assumption of Marcus theory is that the solvent free energy functions controlling ET are paraboli with

equal curvatures (linear response). This leads to an expression for ΔG^* ,which, neglecting surface adsorption and desorption work terms, is given by

$$\Delta G^* = \frac{\left(\lambda + \Delta G_{rxn}\right)^2}{4\lambda} \quad , \tag{14}$$

where the reorganization free energy λ is the reversible work needed to change the solvent configuration from an equilibrium state around the reactants to that around the products at a fixed electronic state. Surface effects are most likely to influence the rate through their effect on λ. This quantity was first calculated analytically by Kharkats (93) for the case of two reactants located along the line normal to the interface (modeled as a continuum dielectric jump). Marcus generalized the calculations to include any orientation of the reactants relative to the interface normal (89). Kharkats and Benjamin (94) investigated the case where the reactants (modeled as spherical cavities) can have a mixed solvation shell at the interface. They show that the reorganization free energy is significantly affected by the possibility of the ions crossing the interface.

Marcus estimated λ by using the rate constant of the half reaction at the solution/metal interface. This estimate and other assumptions gave reasonable agreement with the experimental rate constant for the reaction between the $Fe(CN)_6^{4-/3-}$ couple in water and for the $Lu(PC)_2^{+/2+}$ (hexacyanoferrate-lutetium biphthalocyanine) couple in DCE (89, 90). With the experimental advances over the last two decades, many more rate constants have been measured. For example, in the SECM technique, one is able to increase significantly the range of the driving force (ΔG_{rxn}) for the ET reactions studied at the L/L interface, which provided a more reliable determination of the reorganization free energy (95). In general, it has been found that the rate constant as a function of

driving force follows Eq. 14, especially when the variation in the driving force is accomplished by changing the redox pair. Several cases reported slower rates when the driving force is increased in the so-called inverted region (96). However, when the driving force is varied by changing the concentration of the supporting electrolyte, complications arise due to the breakdown of the assumption that the potential drop across the interface is steep. Independent tests on the validity of the assumptions underlying the ET theory involve molecular-level description, which we discuss next.

3.3.2. Molecular-level description

Marcus provided expressions for the rate constant of ET at the LL interfaces by assuming that the interface is either a mathematically sharp plane or, at the other extreme, a homogeneous surface region. While the experimental and computational work described earlier favors the sharp interface description, the interface is far from being planar. In particular, simulations suggest that the interface is highly corrugated on the scale of typical donor-acceptor distances. In addition, using the continuum electrostatic model to calculate the activation free energy at the interface could lead to errors similar to those observed in the calculations of the ionic free energy of adsorption: The sharp dielectric discontinuity typically magnifies surface effect. Moreover, ions' tendency to keep part or all of their hydration shell can have a major effect on the value of the activation free energy and on their ability to form an interfacial ion-pair – a precursor for the ET reaction. Because experimental data are not sufficiently detailed or extensive to test the above assumptions, atomistic approaches to interfacial ET have been used to gain insight into the influence of the molecular structure of the interface on the ET rate.

A molecular description of ET at IES may use any of the methodologies developed for studying bulk liquid ET, including the calculation of the reorganization free energy, the relative distributions of donor and acceptor molecules, electronic coupling as a function of distance and orientation, and dynamical solvent effects. Some of these have been reported at LL interfaces.

The calculation of reorganization free energy is based on a sampling of an ET reaction coordinate defined as the energy gap between the two electronic states at fixed nuclear coordinates(97-100):

$$X(\mathbf{r}) = U_P(\mathbf{r}) - U_R(\mathbf{r}) \quad , \tag{15}$$

where U_R and U_P are the potential energies of the reactant state $\psi_R = |\mathrm{O_1R_2}\rangle$ and the product state $\psi_P = |\mathrm{O_2R_1}\rangle$, respectively, and $\mathbf{r}$ represents all the nuclear positions. The solvent free energy associated with solvent fluctuations in the electronic state $\nu = R$ or $\nu = P$ is given by

$$G_\nu(x) = -k_B T \ln P_\nu(x), \quad P_\nu(x) = \langle \delta[X(\mathbf{r}) - x] \rangle_\nu \quad , \tag{16}$$

where $P_\nu(x)$ is the probability that the solvent coordinate X has the value x and $\langle \ldots \rangle_\nu$ is the equilibrium average in the state ν. The reorganization free energies for the reactants and products state are given by:

$$\lambda_R = G_R(\bar{x}_P) - G_R(\bar{x}_R), \quad \lambda_P = G_P(\bar{x}_R) - G_P(\bar{x}_P), \tag{17}$$

where $\bar{x}_\nu = \langle X(\mathbf{r}) \rangle_\nu$ is the equilibrium value of the solvent coordinate in the state ν. Because $\bar{x}_R$ and $\bar{x}_P$ are typically very different, an umbrella sampling procedure is

necessary to compute $G_R(\bar{x}_P)$, as one requires sampling of solvent fluctuations far from equilibrium (98). The activation free energy $\Delta G^{\#}$ is determined from the intersection of $G_P(x)$ and $G_R(x)$. Marcus equation 18 is obtained by assuming that these two functions are paraboli with equal curvature, from which one can easily show that $\lambda = \lambda_R = \lambda_P = \frac{k}{2}\left(\bar{x}_R - \bar{x}_P\right)^2$. Fig. 2 depicts graphically the quantities discussed above.

MD calculations of the solvent free energy curves in bulk water (98, 99, 101, 102), in other systems (103), at the interface between two simple liquids (104), and at the water/self-assembled monolayer interface (105) have generally confirmed that the parabolic assumption (and thus linear response) is quite reasonable. In cases where significant non-linearity was observed, approaches to calculating the activation free energy have been discussed (101, 103).

The solvent free energy curves for the model ET reaction $DA \rightarrow D^+A^-$ at the water/1,2-dichloroethane (DCE) interface were compared to those in bulk water by MD simulations (106). The reactants were modeled as point charges imbedded in Lennard-Jones spheres. At the water/DCE interface, (and to a slightly lesser degree in bulk water), the free energy curves are well described by paraboli. The reorganization free energy calculated by continuum electrostatics (89) using the MD-derived static dielectric constants of water ($\varepsilon_0 = 82.5$) and DCE ($\varepsilon_0 = 10$) and other geometrical parameters, is in good agreement with the MD calculations (106). Interestingly, however, the water contribution to the electrostatic potential at the location of the charge transfer centers is underestimated by the continuum model (due to the neglect of the specific hydration structure), while the DCE contribution is overestimated (107, 108).

3.3.4. *Photoinduced ET at liquid/liquid interfaces*

Photoinduced ET at L/L interfaces can be followed using spectroscopic techniques, which when coupled with electrochemical methods allows in principle for a more accurate determination of fast ET processes. The problem of surface selectivity can be overcome by using total internal reflection (TIR) geometry or by utilizing non-linear optical spectroscopy. For example, a TIR geometry was used by Girault and coworkers to study the potential dependent ET in a TCNQ/ferrocyanide system (109). The rate constant was determined by a measurement of the time-dependence of absorbance in response to potential modulations. Other systems studied include photoinduced ET between a porphyrin dimer and one of the following: TCNQ, ferrocene derivatives and quinones (80, 110). The rate as a function of the net driving force in these systems was consistent with the Marcus model.

Of particular interest is the idea of using a solvent, such as *N,N*-dimethylaniline (DMA), as an electron donor in an interfacial ET, thus limiting complications due to ion transfer and reactants' diffusion. This can lead to ultrafast electron transfer due to the close proximity of the redox pair. Several experiments have provided additional examples of the existence of the Marcus inverted region at liquid interfacial systems (111, 112). Eisenthal and coworkers used SHG (81) to study the ultrafast electron transfer between a photoexcited coumarin (C314*) and a DMA molecule at the water/DMA interface. The electron transfer was monitored by measuring the SHG signal resonant with the C314 $S_0 \rightarrow S_1$ transition or by following the SHG signal resonant with an electronic transition in the DMA radical cation. The fast signal change was attributed to the solvation dynamics of $C314^*$ on the sub-picosecond time scale, followed by ET on a 14-16 ps time

scale. More recently, an experiment using a Sum Frequency Generation (SFG) probe resonant with the C=O vibrational frequency in C314 gave a similar time constant of 16 ±2 ps (82).

This ET rate is (surprisingly) faster by a factor of 2 for the same reaction in bulk DMA. A possible explanation is that the water/DMA interfacial region is less polar than the bulk DMA region, which would result in a smaller reorganization free energy (82). This is unusual since the polarity of the interface tends to lie between the polarity of two bulk phases (44, 113). Support for this was provided by the observation that the surface SHG spectrum of C314 is shifted to the blue relative to the UV spectrum of C314 in bulk DMA and in bulk water.

Molecular dynamics calculations of the reorganization free energy and solvation dynamics in the C314 at water/DMA system gave results in agreement with the experiments (114). The calculations suggest that the rate enhancement at the interface relative to the bulk is likely due to faster solvation dynamics at the interface. This is a case where due to strong coupling, the ET is in the adiabatic regime, and the rate is controlled by solvation dynamics (115-120). For reviews of solvation dynamics at liquid interfaces, see (6, 44).

3.4. Liquid-Liquid Phase Transfer Catalysis and interfacial S_N2 reactions

In liquid-liquid Phase Transfer Catalysis (PTC), a water-soluble reactant is transferred, with the aid of a phase transfer catalyst (typically a quaternary ammonium cation), from an aqueous phase into an organic phase, where it reacts with a water-insoluble reactant. Once complete, the catalyst transfers the water-soluble product to the aqueous phase, and the catalytic cycle repeats. Like the case of an electron transfer, this is

an example of an interfacial reaction coupled to mass transport across the interface. PTC is a "green" chemistry process with applications in pharmaceutical and agrochemical industries, materials science and organic synthesis (121-123)

As an example of a reaction carried out under PTC conditions at the liquid/liquid interface, we consider nucleophilic substitution (S_N2). This reaction involves an anionic reactant and product (like OH^- and Cl^-) and cationic catalysts, and thus it involves the ion transfer and interfacial ion solvation processes discussed above. It is well-known that fast gas-phase S_N2 reactions are significantly slowed down when the reaction is carried out in a polar protic solvent such as water (124-135), and that the rate can be enhanced (relative to aqueous solutions) if the reaction is carried out in a low-polarity, aprotic solvent like chloroform. Thus, a PT catalyst can transfer small water soluble nucleophiles such as OH^- and Cl^- into low-polarity solvents and enable the reaction.

Until recently, theoretical studies of PTC processes were limited to continuum diffusion/kinetic models (121), while theoretical studies of S_N2 reactions were extensively studied in the gas phase and bulk liquids (125, 128, 130, 134, 135), but not at interfaces. The molecular level study of S_N2 reactions under PTC conditions at liquid/liquid interfaces provides an opportunity for exploring how the unique character of the liquid interface region affects chemical reactivity. Specific issues of interest include the following:

1. Experimental studies of S_N2 reactions in bulk non-polar solvents suggest that the hydration state of the nucleophile anion strongly influences its reactivity (136), while the transfer of small hydrophilic ions from water to the organic phase discussed above is

accompanied by some water molecules. How important is the hydration state of the nucleophilic ions for reactions carried out under PTC conditions?

2. Several experimental and theoretical studies suggest strong dependence of the effective solvent polarity on the solute's surface location and orientation (137-141). How would the location and relative orientation of the reactants influence their interfacial reactivity?

3. What role might interface density fluctuations play in determining reactivity?

To address these questions, molecular dynamics simulations were carried out for a simple benchmark symmetric S_N2 reaction, $Cl^- + CH_3Cl \rightarrow CH_3Cl + Cl^-$, at different locations at the water/chloroform interface (142). The reaction was modeled using a simple two-state Empirical Valence Bond (EVB) (125, 130, 143) In this approach, the electronic state of the reactive system is described using two orthonormal valence states, $\psi_1 = Cl{:}^{-}CH_3{-}Cl$ and $\psi_2 = Cl{-}CH_3Cl{:}^{-}$

$$\Psi = c_1\psi_1 + c_2\psi_2 \ , \quad \langle \psi_i | \psi_j \rangle = \delta_{ij} \qquad . \tag{18}$$

The total Hamiltonian in this representation is written as:

$$\hat{H} = \begin{pmatrix} H_{11}(\mathbf{r}_i,\mathbf{r}_d,\mathbf{r}_s) & H_{12}(r_1,r_2,\theta) \\ H_{12}(r_1,r_2,\theta) & H_{22}(\mathbf{r}_i,\mathbf{r}_d,\mathbf{r}_s) \end{pmatrix} \tag{19}$$

$$H_{11} = E_k + H_{11}^0(r_1,r_2,\theta) + U_{ss}(\mathbf{r}_s) + U_{si}(\mathbf{r}_s,\mathbf{r}_i) + U_{sd}(\mathbf{r}_s,\mathbf{r}_d) \quad , \tag{20}$$

where H_{11} and H_{22} are the classical diabatic Hamiltonians describing the system in the states ψ_1 and ψ_2, respectively, however due to the symmetry of the reaction, H_{22} has the same functional form as H_{11} but with the two chlorine atom labels interchanged. These Hamiltonians include the following terms:

E_k – the kinetic energy of all atoms; $H_{11}^0(r_1,r_2,\theta)$ – the gas phase interaction between the Cl^- ion and the CH_3Cl molecule; $U_{ss}(\mathbf{r}_s)$ – the individual solvents and the solvent-solvent potential energies; $U_{si}(\mathbf{r}_s,\mathbf{r}_i)$ – the solvent-ion potential energy; and $U_{sd}(\mathbf{r}_s,\mathbf{r}_d)$ – the solvent –CH_3Cl potential energy. In all these terms, $\mathbf{r}_i$ is the vector position of the Cl^- ion, $\mathbf{r}_d$ is the vector position of the CH_3Cl atoms and $\mathbf{r}_s$ represents the positions of all the solvent atoms. r_1 is the distance between the Cl^- ion and the carbon atom, r_2 is the C-Cl bond distance in CH_3Cl, and θ is the Cl^-----C-Cl angle. The detailed functional forms and parameter values of all these potential energy terms can be found elsewhere (143). The off-diagonal electronic coupling term H_{12} in Eq. 19 is the one suggested by Hynes and coworkers:(130, 144)

$$H_{12} = -QS(r_1)S(r_2) \quad , \tag{21}$$

where $S(r)$ is the overlap integral for the sigma orbital formed from the carbon 2p and chlorine 3p atomic orbitals centered a distance r apart, and Q = 678.0 kcal/mol is a parameter that is fitted to obtain the experimental gas-phase activation energy.

The lower eigenvalue of the Hamiltonian in Eq. 19 gives the classical electronic ground state adiabatic Hamiltonian as a function of all nuclear coordinates:

$$H_{ad} = \frac{1}{2}(H_{11}+H_{22}) - \frac{1}{2}\left[(H_{11}-H_{22})^2 + 4H_{12}^2\right]^{1/2} \quad . \tag{22}$$

The classical MD calculations are carried out using this as the total system Hamiltonian.

(Note that if the coupling is zero, the Hamiltonian is reduced to one of the diabatic states.) The reaction coordinate is defined by

$$\xi = r_1 - r_2 \quad , \tag{23}$$

so the reactant and product states correspond to $\xi << 0$ and $\xi >> 0$, respectively. The minimum energy path along ξ for the collinear geometry ($\theta = 0$) is shown in Fig. 3. The system's electronic wavefunction (the values for c_1 and c_2 in Eq. 18) shows that at the transition state in a vacuum (and on average in solution) each Cl atom in the reaction system carries a partial charge of $\delta \approx 0.5$: $\left[Cl^{-\delta} - CH_3 - Cl^{-\delta}\right]$. As ξ varies from $-\infty$ to $+\infty$, the charge on the nucleophile varies, as expected, from -1 to the charge on the Cl atom in the isolated CH_3Cl molecule.

The reaction free energy profile as a function of the reaction coordinate $W(\xi)$ (from which one can obtain the activation free energy and estimate the rate) can be calculated using umbrella sampling with overlapping windows with the help of a biasing potential to accelerate convergence(145) according to:

$$W(\xi) = -\beta^{-1} \ln P(\xi) - U_b(\xi) \tag{24}$$

$$P(\xi) = \frac{\int \delta(r_1 - r_2 - \xi) \exp\left[-\beta(H_{ad} + U_b(\xi)\right] d\Gamma}{\int \exp[-\beta(H_{\text{ad}} + U_b(\xi)] d\Gamma} \quad . \tag{25}$$

The biasing potential $U_b(\xi)$ is any analytic function of ξ chosen to approximate $-W(\xi)$. The $W(\xi)$ was calculated at 7 different interface locations by restricting the reactants'

center of mass to slabs parallel to the liquid/liquid interface. Other details about the calculations are given elsewhere (143).

Some results are shown in Fig. 3. The top panel shows the gas-phase potential energy along the minimum energy path for the collinear reaction geometry (dotted line), the free energy profiles in bulk chloroform and in bulk water, and the free energy profiles at two interface locations. The bottom panel shows the activation free energy barrier (ΔA^*) for all the locations studied vs. the distance along the interface normal. Upon transferring from the gas phase to bulk chloroform and bulk water, the increase in solvent polarity gives rise to increased stabilization of the localized charges of the reactants and products (on the chloride ion) compared with the delocalized charges at the transition state, leading to the observed increase in ΔA^*. As the polarity of the interface region is expected to be somewhere between that of the two bulk phases (113, 146), one would expect that ΔA^* at different interface locations will fall in between the values in bulk water and bulk chloroform. Unexpectedly, the bottom panel of Fig. 5 shows that ΔA^* at the Gibbs surface ($Z = 0$) is larger than in bulk water. As the reactants' center of mass moves towards the organic phase, ΔA^* further *increases*, reaches a maximum near $Z \approx 5$ Å, and is still higher than in bulk chloroform at the largest Z value studied.

The surprising behavior described above is a direct consequence of the structure of the interface and the behavior of ionic solute at the interface discussed in the first part of this review. Interface density fluctuations are strongly coupled to the solute charge distribution (and thus to the reaction coordinate) due to the ability of the nucleophile to retain some number of water molecules when it is near the interface. This helps to understand the behavior of the reactants in the region $Z > 5$Å. In this case, the behavior is

similar to that of the reaction $Cl^-(H_2O)_n + CH_3Cl$ in bulk chloroform. For example, at Z = 15Å, ΔA^* = 22 kcal/mol, which is similar to ΔA^* = 21 kcal/mol calculated for the reaction in bulk chloroform with n = 1. As n increases, the activation free energy increases monotonically to the value in bulk water (147). However, when the reactants are near the Gibbs surface another effect is at play, which is related to the dependence of the reaction barrier on the reactants' orientation (142). When the system is at or near the transition state ($\xi = 0$), the $Cl^{-0.5} - CH_3 - Cl^{-0.5}$ vector tends to lie *parallel* to the interface, but when the charge on the nucleophile is near -1 (at $\xi \geq 0.3$Å), the vector $Cl^- - -CH_3 - Cl$ tends to lie *perpendicular* to the interface, with the Cl^- pointing towards the water phase. As a result, the transition state experiences an environment that is significantly less polar than the environment experienced by the reactants, explaining the high barrier in the $Z < 5$ Å region.

These results suggest that for the phase transfer catalyst to be effective, it must be able to bring the nucleophile relatively deep into the organic phase. A question remains: To what extent does the catalyst influence the reaction itself? Calculations were performed of the free energy profile of the benchmark Cl^- + CH_3Cl S_N2 reaction at the water/chloroform interface in the presence of the phase transfer catalyst tetramethylammonium cation (TMA^+) (148). It was found that TMA^+ moderately *increases* the barrier height of this reaction when it is still paired with the Cl^- nucleophile, especially when the nucleophile is hydrated by a few water molecules. A design principle for a good phase transfer catalyst is thus the ability to bring the

nucleophile into the organic phase with a minimal number of associated water molecules, followed by dissociation of the ion pair in the bulk organic phase before reaction (72).

4. Conclusions

The interface between two fluid phases is a few nm thick, highly anisotropic region, characterized by rapidly varying density, polarity and molecular structure. Density fluctuations create instantaneous structures that are significant on the interface length scale. These have marked influence on the solvation of solute molecules and on the equilibrium and rate of chemical reactions. In some cases, the effect of the interface region can be understood by the direct application of theories developed for understanding solvation and reactivity in bulk liquids. For example, by introducing the concept of interface polarity, one can understand the solvent effect on the rate of electron transfer reactions. In other cases, unique interface structures must be considered in order to explain surface effects. For example, surface roughness at the interface between two immiscible liquids can have a significant effect on the activation free energy for S_N2 reactions. An important concept that is emerging from many simulation studies and is also supported by experimental evidence is the ability of a charged solute to keep a hydration shell (to a degree that depends on the solute's charge and size) as it crosses the interface between water and a second phase. This has an important effect on many thermodynamic and dynamic properties of reactive solutes adsorbed at the interface.

ACKNOWLEDGEMENT

This work was supported by the National Science Foundation (grant CHE-0809164). I would like to thank my collaborators: Prof. Mark Schlossman, Daniel Rose, Karl Schweighofer, David Michael, Ilya Chorny, John Vieceli Nicholas Winter and Katherine Nelson.

LITERATURE CITED

1. Adamson AW. 1990. *Physical Chemistry of Surfaces*. New York: Wiley
2. Girault HH, Schiffrin DJ. 1989. Electrochemistry of liquid-liquid interfaces. In *Electroanalytical Chemistry*, ed. AJ Bard:1. New York: Dekker.
3. Shen YR. 1989. Surface properties probed by 2nd harmonic and sum frequency generation. *Nature* 337:519-25
4. Eisenthal KB. 1996. Liquid interfaces by second harmonic and sum-frequency spectroscopy. *Chem. Rev.* 96:1343
5. Richmond GL. 2002. Molecular bonding and interactions at aqueous surfaces as probed by vibrational sum frequency spectroscopy. *Chem. Rev.* 102:2693
6. Eisenthal KB. 2006. Second harmonic spectroscopy of aqueous nano- and microparticle interfaces. *Chem. Rev.* 106:1462-77
7. Geiger FM. 2009. Second harmonic generation, sum frequency generation, and $\chi^{(3)}$: Dissecting environmental interfaces with a nonlinear optical swiss army knife. *Annu. Rev. Phys. Chem.* 60:61-83

8. Pomfret MB, Owrutsky JC, Walker RA. 2010. In situ optical studies of solid-oxide fuel cells. *Ann. Rev. Anal. Chem.* 3:151-74

9. Schlossman ML. 2002. Liquid-liquid interfaces: studied by X-ray and neutron scattering. *Curr. Opin. Coll. Interf. Sci.* 7:235-43

10. Luo G, Malkova S, Pingali SV, Schultz DG, Lin B, et al. 2005. X-ray studies of the interface between two polar liquids: neat and with electrolytes. *Faraday Discuss* 129:23-34; discussion 89-109

11. Bard AJ, Mirkin MV, eds. 2001. *Scanning Electrochemical Microscope*. New York: Marcel Dekker.

12. Henderson D, ed. 1992. *Fundamentals of Inhomogeneous Fluids*. New York: Marcel Dekker.

13. Benjamin I. 1997. Molecular structure and dynamics at liquid-liquid interfaces. *Annu. Rev. Phys. Chem.* 48:401

14. Pratt LR, Pohorille A. 2002. Hydrophobic effects and modeling of biophysical aqueous solution interfaces. *Chem. Rev.* 102:2671-91

15. Chang TM, Dang LX. 2006. Recent advances in molecular simulations of ion solvation at liquid interfaces. *Chem. Rev.* 106:1305-22

16. Jungwirth P, Tobias DJ. 2006. Specific ion effects at the air/water interface. *Chem. Rev.* 106:1259-81

17. Schoen M, Klapp SHL. 2007. Nanoconfined fluids: soft matter between two and three dimensions. In *Reviews in Computational Chemistry*, ed. KB Lipkowitz, DB Boyd, 24:1-509.

18. Rowlinson JS, Widom B. 1982. *Molecular Theory of Capillarity*. Oxford: Clarendon

19. Luo G, Malkova S, Yoon J, Schultz DG, Lin B, et al. 2006. Ion distributions near a liquid-liquid interface. *Science* 311:216

20. Luo G, Malkova S, Yoon J, Schultz DG, Lin B, et al. 2006. Ion distributions at the nitrobenzene-water interface electrified by a common ion. *J. Electroanal. Chem.* 593:142-58

21. Darve E, Pohorille A. 2001. Calculating free energies using average force. *J. Chem. Phys.* 115:9169-83

22. Petersen PB, Saykally RJ. 2006. On the nature of ions at the liquid water surface. *Annu. Rev. Phys. Chem.* 57:333-64

23. *R.Vácha*, *Uhlig F*, *Jungwirth P*. 2014. Charges at aqueous interfaces: Development of computational approaches in direct contact with experiment *Adv. Chem. Phys.* 155:69-96

24. Nagatani H, Harada M, Tanida H, Sakae H, Imura H. 2014. Communication: Coordination structure of bromide ions associated with hexyltrimethylammonium cations at liquid/liquid interfaces under potentiostatic control as studied by total-reflection X-ray absorption fine structure. *J. Chem. Phys.* 140

25. Wilson MA, Pohorille A. 1991. Interaction of monovalent ions with the water liquid-vapor: A molecular dynamics study. *J. Chem. Phys.* 95:6005

26. Benjamin I. 1991. Theoretical study of ion solvation at the water liquid-vapor interface. *J. Chem. Phys.* 95:3698

27. Dang LX. 2002. Computational study of ion binding to the liquid interface of water. *J. Phys. Chem. B* 106:10388-94

28. Chorny I, Benjamin I. 2005. Hydration shell exchange dynamics during ion transfer across the liquid/liquid interface. *J Phys Chem B* 109:16455-62

29. Wick CA, Xantheas SS. 2009. Computational Investigation of the First Solvation Shell Structure of Interfacial and Bulk Aqueous Chloride and Iodide Ions. *J. Phys. Chem. B* 113:4141-6

30. Warren GL, Patel S. 2008. Comparison of the solvation structure of polarizable and nonpolarizable ions in bulk water and near the aqueous liquid-vapor interface. *J. Phys. Chem. C* 112:7455-67

31. Uhlig F, Marsalek O, Jungwirth P. 2013. Electron at the surface of water: Dehydrated or not? *J. Phys. Chem. Lett*. 4:338-43

32. Benjamin I. 1993. Mechanism and dynamics of ion transfer across a liquid-liquid interface. *Science* 261:1558-60

33. Schweighofer KJ, Benjamin I. 1995. Transfer of small ions across the water/1,2-dichloroethane interface. *J. Phys. Chem.* 99:9974

34. Dang LX. 1999. Computer simulation studies of ion transport across a liquid/liquid interface. *J. Phys. Chem. B* 103:8195-200

35. Schweighofer KJ, Benjamin I. 1999. Transfer of a tetra methyl ammonium ion across the water-nitrobenzene interface: Potential of mean force and non-equilibrium dynamics. *J. Phys. Chem. A* 103:10274-9

36. Wick CD, Dang LX. 2006. Distribution, structure, and dynamics of cesium and iodide ions at the H_2O-CCl_4 and H_2O-vapor interfaces. *J. Phys. Chem. B* 110:6824-31

37. Wick CD, Dang LX. 2008. Molecular dynamics study of ion transfer and distribution at the interface of water and 1,2-dichlorethane. *J. Phys. Chem. C* 112:647-9

38. Wick CD, Dang LX. 2008. Recent advances in understanding transfer ions across aqueous interfaces. *Chem. Phys. Lett.* 458:1-5

39. Benjamin I. 2008. Structure and dynamics of hydrated ions in a water-immiscible organic solvent. *J Phys Chem B* 112:15801-6

40. Wick CD, Cummings OT. 2011. Understanding the factors that contribute to ion interfacial behavior. *Chem. Phys. Lett.* 513:161-6

41. Noah-Vanhoucke J, Geissler PL. 2009. On the fluctuations that drive small ions toward, and away from, interfaces between polar liquids and their vapors. *Proc. Nat. Acad. Sci. U. S. A.* 106:15125-30

42. Vieceli J, Chorny I, Benjamin I. 2002. Vibrational relaxation at water surfaces. *J. Chem. Phys.* 117:4532

43. Chorny I, Benjamin I. 2004. Molecular dynamics study of the vibrational relaxation of OCl and OCl^- in the bulk and the surface of water and acetonitrile. *J. Mol. Liq.* 110:133-9

44. Benjamin I. 2006. Static and dynamic electronic spectroscopy at liquid interfaces. *Chem. Rev.* 106:1212-33

45. Benjamin I. 2009. Solute dynamics at aqueous interfaces. *Chem. Phys. Lett.* 469:229-41

46. Chandler D. 1978. Statistical mechanics of isomerization dynamics in liquids and the transition state approximation. *J. Chem. Phys.* 68:2959

47. Hynes JT. 1985. The theory of reactions in solution. In *The Theory of Chemical Reactions*, ed. M Baer, 4:171. Boca Raton, FL: CRC Press.

48. Berne BJ, Borkovec M, Straub JE. 1988. Classical and modern methods in reaction rate theory. *J. Phys. Chem.* 92:3711

49. Whitnell RM, Wilson KR. 1993. Computational molecular dynamics of chemical reactions in solution. In *Reviews in Computational Chemistry*, ed. KB Lipkowitz, DB Boyd, 4:67-148 New York: VCH.

50. Fleming GR. 1986. *Chemical Applications of Ultrafast Spectroscopy*. New York: Oxford University

51. Benjamin I. 2002. Chemical reaction dynamics at liquid interfaces. A computational approach. *Prog. React. Kin. Mech.* 27:87-126

52. Wang SZ, Bianco R, Hynes JT. 2011. An atmospherically relevant acid: HNO_3. *Comput Theor Chem* 965:340-5

53. Volkov AG, Deamer DW, eds. 1996. *Liquid-Liquid Interfaces*. Boca Raton: CRC press.

54. Dryfe RAW. 2009. The Electrified Liquid-Liquid Interface. *Adv. Chem. Phys.* 141:153-215

55. Mirkin MV, Tsionsky M. 2012. Charge transfer processes at the liquid-liquid interface. In *Scanning Electrochemical Microscopy*, ed. AJ Bard, MV Mirkin:191-231: CRC Press.

56. Vallejo LJS, Ovejero JM, Fern´andez RA, Dassie SA. 2012. Simple ion transfer at liquid|liquid interfaces. *Int. J. Electrochem.* 2012:1-35

57. Scholz F. 2006. Recent advances in the electrochemistry of ion transfer processes at liquid–liquid interfaces. *Annu. Rep. Prog. Chem. Sect. C* 102:43-70

58. Pohorille A, Cieplak P, Wilson MA. 1996. Interactions of anesthetics with the membrane-water interface. *Chem. Phys.* 204:337

59. Chipot C, Wilson MA, Pohorille A. 1997. Interactions of anesthetics with the water-hexane interface. A molecular dynamics study. *J. Phys. Chem. B* 101:782-91

60. Wick CD, Dang LX. 2008. Molecular dynamics study of ion transfer and distribution at the interface of water and 1,2-dichlorethane. *J. Phys. Chem. C.* 112:647-9

61. Kikkawa N, Ishiyama T, Morita A. 2012. Molecular dynamics study of phase transfer catalyst for ion transfer through water-chloroform interface. *Chem. Phys. Lett.* 534:19-22

62. Levin Y, dos Santos AP, Diehl A. 2009. Ions at the air-water interface: An end to a hundred-year-old mystery? *Phys. Rev. Lett.* 103

63. Rose D, Benjamin I. 2009. Free energy of transfer of hydrated ion clusters from water to an immiscible organic solvent *J. Phys. Chem. B* 113:9296-303

64. Britz D. 2005. *Digital Simulation in Electrochemistry*. Berlin Hiedelberg: Springer

65. Benjamin I. 1992. Dynamics of ion transfer across a liquid-liquid interface: A comparison between molecular dynamics and a diffusion model. *J. Chem. Phys.* 96:577

66. Kakiuchi T. 1992. Current potential characteristic of ion transfer across the interface between 2 Immiscible electrolyte-solutions based on the Nernst-Planck equation. *J. Electroanal. Chem.* 322:55-61

67. Schmickler W. 1997. A model for ion transfer through liquid|liquid interfaces. *J. Electroanal. Chem.* 426:5-9

68. Holmberg N, Sammalkorpi M, Laasonen K. 2014. Ion Transport through a Water-Organic Solvent Liquid-Liquid Interface: A Simulation Study. *J. Phys. Chem. B* 118:5957-70

69. Marcus RA. 2000. On the theory of ion transfer rates across the interface of two immiscible liquids. *J. Chem. Phys.* 113:1618-29

70. Kornyshev AA, Kuznetsov AM, Urbakh M. 2002. Coupled ion-interface dynamics and ion transfer across the interface of two immiscible liquids. *J. Chem. Phys. (USA)* 117:6766-79

71. Verdes CG, Urbakh M, Kornyshev AA. 2004. Surface tension and ion transfer across the interface of two immiscible electrolytes. *Electrochem Commun* 6:693-9

72. Benjamin I. 2013. Recombination, dissociation and transport of ion pairs across the liquid/liquid interface. Implications for phase transfer catalysis. *J. Phys. Chem. A* 117:4325-31

73. Laforge FO, Sun P, Mirkin MV. 2006. Shuttling Mechanism of ion transfer at the interface between two immiscible liquids. *J. Am. Chem. Soc.* 128:15019-25

74. Lahtinen R, Fermin DJ, Kontturi K, Girault HH. 2000. Artificial photosynthesis at liquid vertical bar liquid interfaces: photoreduction of benzoquinone by water soluble porphyrin species. *J. Electroanal. Chem.* 483:81-7

75. Barbara PF, Olson EJJ. 1999. Experimental electron transfer kinetics in a DNA environment. *Adv. Chem. Phys.* 107:647-76

76. Wei C, Bard AJ, Mirkin MV. 1995. Scanning electrochemical microscopy .31. Application of SECM to the study of charge-transfer processes at the liquid-liquid interface. *J. Phys. Chem.* 99:16033-42

77. Shi C, Anson FC. 1999. Electron transfer between reactants located on opposite sides of liquid/liquid interfaces. *J. Phys. Chem. B.* 103:6283-9

78. Fermin DJ, Duong HD, Ding Z, Brevet P-F, Girault HH. 1999. Photoinduced electron transfer at liquid/liquid interfaces. Part III. Photoelectrochemical responses involving porphyrin ion pairs. *J. Am. Chem. Soc.* 121:10203-10

79. Jensen H, Fermin DJ, Girault HH. 2001. Photoinduced electron transfer at liquid/liquid interfaces. Part V. Organisation of water-soluble chlorophyll at the water/1,2-dichloroethane interface. *Phys. Chem. Chem. Phys.* 3:2503-8

80. Eugster N, Fermin DJ, Girault HH. 2003. Photoinduced electron transfer at liquid|liquid interfaces: dynamics of the heterogeneous photoreduction of quinones by self-assembled porphyrin ion pairs. *J. Am. Chem. Soc.* 125:4862-9

81. McArthur EA, Eisenthal KB. 2006. Ultrafast excited-state electron transfer at an organic liquid/aqueous interface. *J. Am. Chem. Soc.* 128:1068-9

82. Rao Y, Xu M, Jockusch S, Turro NJ, Eisenthal KB. 2012. Dynamics of excited state electron transfer at a liquid interface using time-resolved sum frequency generation. *Chem. Phys. Lett.* 544:1-6

83. Marcus RA. 1965. On the theory of electron-transfer reactions. VI. Unified treatment for homogeneous and electrode reactions. *J. Chem. Phys.* 43:679

84. Ulstrup J. 1979. *Charge Transfer Processes in Condensed Media*. Berlin: Springer

85. Newton MD, Sutin N. 1984. Electron transfer reactions in condensed phases. *Ann. Rev. Phys. Chem.* 35:437

86. Weaver MJ. 1992. Dynamical solvent effects on activated electron-transfer reactions: principles, pitfalls, and progress. *Chem. Rev.* 92:463

87. Shi C, Anson FC. 2001. Rates of electron-transfer across liquid/liquid interfaces. effects of changes in driving force and reaction reversibility. *J. Phys. Chem. B.* 105:8963-9

88. Schmickler W. 1997. Electron-transfer reactions across liquid/liquid interfaces. *J. Electroanal. Chem.* 428:123-7

89. Marcus RA. 1990. Reorganization free energy for electron transfers at liquid-liquid and dielectric semiconductor-liquid interfaces. *J. Phys. Chem.* 94:1050-5

90. Marcus RA. 1990. Theory of electron-transfer rates across liquid-liquid interfaces. *J. Phys. Chem.* 94:4152-5

91. Marcus RA. 1991. Theory of electron-transfer rates across liquid-liquid interfaces. 2. Relationships and Application. *J. Phys. Chem.* 95:2010-3

92. Wittig C. 2005. The Landau-Zener formula. *J. Phys. Chem. B* 109:8428-30

93. Kharkats YI. 1976. On the calculation of probability of electron transfer through the interface between two dielectric media. *Elektrokhimiya* 12:1370

94. Benjamin I, Kharkats YI. 1998. Reorganization free energy for electron transfer reactions at liquid/liquid interfaces. *Electrochimica Acta* 44:133-8

95. Li F, Whitworth AL, Unwin PR. 2007. Measurement of rapid electron transfer across a liquid/liquid interface from 7,7,8,8-tetracyanoquinodimethane radical anion in 1,2-dichloroethane to aqueous tris(2,2-bipyridyl)-ruthenium (III). *J. Electroanal. Chem.* 602:70-6

96. Ding Z, Quinn BM, Bard AJ. 2001. Kinetics of heterogeneous electron transfer at liquid/liquid interfaces as studied by SECM. *J. Phys. Chem. B.* 105:6367-74

97. Hwang JK, Warshel A. 1987. Microscopic examination of free-energy relationships for electron transfer in polar solvents. *J. Am. Chem. Soc.* 109:715-20

98. King G, Warshel A. 1990. Investigation of the free energy functions for electron transfer reactions. *J. Chem. Phys.* 93:8682-92

99. Kuharski RA, Bader JS, Chandler D, Sprik M, Klein ML, Impey RW. 1988. Molecular model for aqueous ferrous-ferric electron transfer. *J. Chem. Phys.* 89:3248-57

100. Carter EA, Hynes JT. 1989. Solute-dependent solvent force constants for ion pairs and neutral pairs in polar solvent. *J. Phys. Chem.* 93:2184-7

101. Matyushov DV, Voth GA. 2000. Modeling the free energy surfaces of electron transfer in condensed phases. *J. Chem. Phys.* 113:5413-24

102. Small DW, Matyushov DV, Voth GA. 2003. The theory of electron transfer reactions: What may be missing? *J. Am. Chem. Soc.* 125:7470

103. Matyushov DV. 2007. Energetics of electron-transfer reactions in soft condensed media. *Acc. Chem. Res.* 40:294-301

104. Benjamin I. 1991. Molecular dynamics study of the free energy functions for electron transfer reactions at the liquid-liquid interface. *J. Phys. Chem.* 95:6675-83

105. Vieceli J, Benjamin I. 2004. Electron transfer at the interface between water and self-assembled monolayers. *Chem. Phys. Lett.* 385:79-84

106. Benjamin I. 1994. A molecular model for an electron transfer reaction at the water/1,2-dichloroethane interface. In *Structure and Reactivity in Aqueous Solution: ACS Symposium series 568*, ed. CJ Cramer, DG Truhlar:409. Washington, D. C.: American Chemical Society.

107. Benjamin I. 1994. Solvation and charge transfer at liquid interfaces. In *Reaction Dynamics in Clusters and Condensed Phases*, ed. J Jortner, RD Levine, B Pullman:179. Dordrecht, The Netherlands: Kluwer.

108. Benjamin I. 1995. Theory and computer simulations of solvation and chemical reactions at liquid interfaces. *Acc. Chem. Res.* 28:233

109. Ding ZF, Fermin DJ, Brevet PF, Girault HH. 1998. Spectroelectrochemical approaches to heterogeneous electron transfer reactions at the polarised water vertical bar 1,2-dichloroethane interfaces. *J. Electroanal. Chem.* 458:139-48

110. Eugster N, Fermin DJ, Girault HH. 2002. Photoinduced electron transfer at liquid/liquid interfaces. Part VI. On the thermodynamic driving force dependence of the phenomenological electron-transfer rate constant. *J. Phys. Chem. B* 106:3428-33

111. Chakraborty A, Seth D, Setua P, Sarkar N. 2006. Photoinduced electron transfer from N,N-dimethylaniline to 7-amino Coumarins in protein-surfactant complex: Slowing down of electron transfer dynamics compared to micelles. *J. Chem. Phys.* 124:074512-21

112. Ghosh S, Mondal SK, Sahu K, Bhattacharyya K. 2007. Ultrafast photoinduced electron transfer from dimethylaniline to coumarin dyes in sodium dodecyl sulfate and triton X-100 micelles. *J. Chem. Phys.* 126:204708-18

113. Wang HF, Borguet E, Eisenthal KB. 1998. Generalized interface polarity scale based on second harmonic spectroscopy. *J. Phys. Chem. B* 102:4927-32

114. Cooper JK, Benjamin I. 2014. Photoinduced excited state electron transfer at liquid/liquid interfaces. *J. Phys. Chem. B* ASAP

115. Maroncelli M. 1993. The dynamics of solvation in polar liquids. *J. Mol. Liq* 57:1

116. Rossky PJ, Simon JD. 1994. Dynamics of chemical processes in polar solvents. *Nature* 370:263

117. Stratt RM, Maroncelli M. 1996. Nonreactive dynamics in solution: the emerging molecular view of solvation dynamics and vibrational relaxation. *J. Phys. Chem.* 100:12981

118. Nandi N, Bhattacharyya K, Bagchi B. 2000. Dielectric relaxation and solvation dynamics of water in complex chemical and biological systems. *Chem. Rev.* 100:2013

119. Bagchi B, Jana B. 2010. Solvation dynamics in dipolar liquids. *Chem. Soc. Rev.* 39:1936-54

120. Thompson WH. 2011. Solvation dynamics and proton transfer in nanoconfined liquids. *Ann. Rev. Phys. Chem.* 62:599-619

121. Makosza M. 2000. Phase transfer catalysis. A general green methodology in organic synthesis. *Pure Appl. Chem.* 72:1399-403

122. Volkov AG, ed. 2003. *Interfacial Catalysis*. New York: Marcel Dekker.

123. Eckert CA, Liotta CL, Bush D, Brown JS, Hallett JP. 2004. Sustainable reactions in tunable solvents. *J. Phys. Chem. B.* 108:18108-18

124. Ingold CK. 1969. *Structure and Mechanism in Organic Chemistry*. Ithaca, NY: Cornell University

125. Warshel A, Weiss RM. 1980. An empirical valence bond approach for comparing reactions in solutions and in enzymes. *J. Am. Chem. Soc.* 102:6218

126. Hwang JK, King G, Creighton S, Warshel A. 1988. Simulation of free-energy relationships and dynamics of S_N2 reactions in aqueous-solution. *J. Am. Chem. Soc.* 110:5297-311

127. Chandrasekhar J, Smith SF, Jorgensen WL. 1984. S_N2 reaction profiles in the gas-phase and aqueous-solution. *J. Am. Chem. Soc.* 106:3049-50

128. Jorgensen WL, Buckner JK. 1986. Effect of hydration on the structure of an S_N2 transition-state. *J. Phys. Chem.* 90:4651-4

129. Reichardt C. 1988. *Solvents and Solvent Effects in Organic Chemistry*. Weinheim: Springer-Verlag

130. Mathis JR, Bianco R, Hynes JT. 1994. On the activation free-energy of the Cl^- $+CH_3Cl$ S_N2 reaction in solution. *J. Mol. Liq.* 61:81-101

131. Hu W-P, Truhlar DG. 1994. Modeling transition state solvation at the single-molecule level: Test of sorrelated ab initio predictions against experiment for the Gas-Phase S_N2 reaction of microhydrated fluoride with methyl chloride. *J. Am. Chem. Soc.* 116:7797-800

132. Vayner G, Houk KN, Jorgensen WL, Brauman JI. 2004. Steric retardation of S_N2 reactions in the gas phase and solution. *J. Am. Chem. Soc.* 126:9054-8

133. Almerindo GI, Pliego JR. 2006. Rate acceleration of S_N2 reactions through selective solvation of the transition state. *Chem. Phys. Lett.* 423:459-62

134. Pliego JR. 2009. First solvation shell effects on ionic chemical reactions: New Insights for supramolecular catalysis. *J Phys Chem B* 113:505-10

135. Kim Y, Cramer CJ, Truhlar DG. 2009. Steric effects and solvent effects on S_N2 reactions. *J. Phys. Chem. A* 113:9109

136. Albanese D, Landini D, Maia A, Penso M. 2001. Key role of water for nucleophilic substitutions in phase-transfer-catalyzed processes: A mini-review. *Ind Eng Chem Res* 40:2396-401

137. Tamburello-Luca AA, Hébert P, Antoine R, Brevet PF, Girault HH. 1997. Optical surface second harmonic generation study of the two acid/base equilibria of Eosin B at the air/water interface. *Langmuir* 13:4428-34

138. Steel WH, Walker RA. 2003. Solvent polarity at an aqueous/alkane interface: The effect of solute identity. *J. Am. Chem. Soc.* 125:1132-3

139. Steel WH, Walker RA. 2003. Measuring dipolar width across liquid-liquid interfaces with 'molecular rulers'. *Nature* 424:296-9

140. Steel WH, Lau YY, Beildeck CL, Walker RA. 2004. Solvent polarity across weakly associating interfaces. *J. Phys. Chem. B* 108:13370-8

141. Steel WH, Beildeck CL, Walker RA. 2004. Solvent polarity across strongly associating interfaces. *J. Phys. Chem. B* 108:16107-16

142. Nelson KV, Benjamin I. 2010. A molecular dynamics-empirical valence bond study of an S_N2 reaction at the water/chloroform interface. *J. Phys. Chem. C.* 114:1154-63

143. Benjamin I. 2008. Empirical valence bond model of an S_N2 reaction in polar and non-polar solvents. *J. Chem. Phys.* 129:074508

144. Timoneda JJI, Hynes JT. 1991. Nonequilibrium free-energy surfaces for hydrogen-bonded proton-transfer complexes in solution. *J. Phys. Chem.* 95:10431-42

145. Chandler D. 1987. *Introduction to Modern Statistical Mechanics*. Oxford: Oxford University Press

146. Benjamin I. 1998. Solvent effects on electronic spectra at liquid interfaces. A continuum electrostatic model. *J. Phys. Chem. A* 102:9500

147. Nelson KV, Benjamin I. 2009. Microhydration effects on a model S_N2 reaction in a nonpolar solvent. *J. Chem. Phys.* 130:194502

148. Nelson KV, Benjamin I. 2011. Effect of a phase transfer catalyst on the dynamics of an S_N2 reaction. A molecular dynamics study. *J. Phys. Chem. C* 115:2290-6

Figure Captions

Fig. 1. The relative (to the bulk) number of water molecules in the first solvation shell of different ions and neutral atoms as a function of the distance from the interface.

Fig. 2. A schematic representation of the free energy functions for the thermally activated electron transfer reaction $O_1(w) + R_2(o) \rightleftarrows R_1(w) + O_2(o)$

Fig. 3. Top: The free energy profile (kcal/mol) for the Cl^- + CH_3Cl reaction at two different locations of the water/chloroform interface (red lines labeled a and b), in bulk water (blue line labeled H_2O) and in bulk chloroform (green line labeled $CHCl_3$). The dotted line is the minimum energy path along the collinear geometry in the gas phase. Bottom: The activation free energy (kcal/mol) vs. the distance along the interface normal. Reprinted with permission from reference 142. Copyright 2010, American Chemical Society.

Table 1. Calculated ratios of bulk to surface peak values of the radial distribution functions for different solute molecules at the liquid/vapor interface of water and acetonitrile at 298K (42, 43).

solute	solvent	$g_{\max}^{\text{bulk}} / g_{\max}^{\text{surf}}$
I_2^-	H_2O	1.6
I_2	H_2O	3.0
ClO	H_2O	3.2
ClO^-	H_2O	1.2
ClO	CH_3CN	2.8
ClO^-	CH_3CN	1.0

Fig. 1

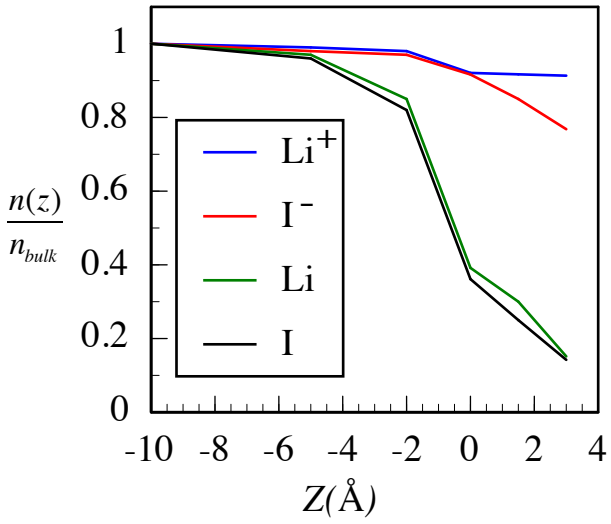
1
0.8
0.6
0.4
0.2
0
n(z)
n_bulk
Li+
I−
Li
I
-10
-8
-6
-4
-2
0
2
4
Z(Å)

Fig. 2.

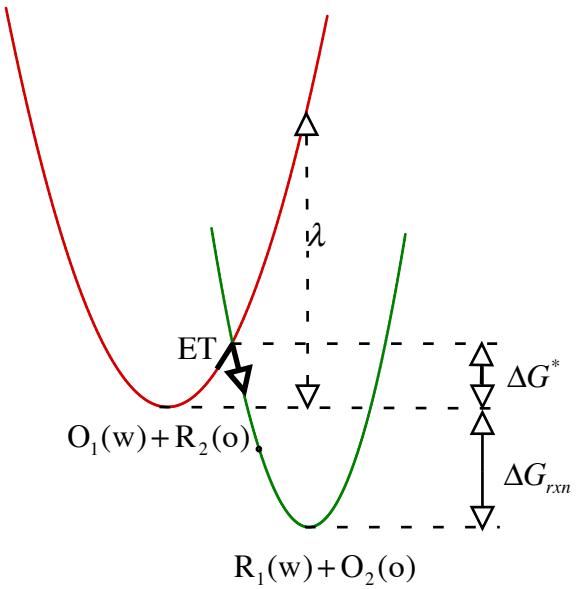
λ
ET
ΔG*
O1(w) + R2(o)
ΔGrxn
R1(w) + O2(o)

Fig. 3.